Int. J. Electrochem. Sci., 7 **(2012)** 965 - 978

International Journal of
ELECTROCHEMICAL
SCIENCE
www.electrochemsci.org

Construction of Sensitive Amperometric Immunosensor Based on Poly(amidoamine) Dendrimer and One-step Ionic-liquid-assisted Graphene/Chitosan Platform for Benzo[a]pyrene Detection

Mouhong Lin, Yingju Liu[*]*, Zhuohong Yang, Yibin Huang, Zihong Sun, Yuan He, Chunlin Ni*[*]

Institute of Biomaterials, College of Sciences, South China Agricultural University, Guangzhou 510642, Guangdong Province, China
[*]E-mail: liuyingju@hotmail.com; niclchem@scau.edu.cn

Received: 21 November 2011 / *Accepted:* 30 December 2011 / *Published:* 1 February 2012

A novel electrochemical immunosensor was proposed using a poly(amidoamine) dendrimer (PAMAM) modified ionic-liquid-assisted graphene sheets-doped chitosan (GS-CS) hybrid matrix as platform, which were characterized by cyclic voltammograms and scanning electron microscopy. Subsequently, using benzo[a]pyrene (BaP) as a model, a competitive immunoreaction between BaP antigen (BaP-Ag) on the platform and the analyte in testing solution was developed to combine with the limited antibody. Results showed that a rapid and sensitive detection of BaP can be found in the range from 5 nM to 6 μM with a low detection limit of 3 nM. Such greatly enhanced sensitivity was based on a two-step signal amplification strategy during the fabrication of the sensor platform: firstly, the addition of ionic-liquid-assisted graphene enlarged the surface area of the substrate and improved the conductivity by favoring electron communication between biomolecules and the substrate. Secondly, the introduction of PAMAM can greatly amplify binding sites of the substrate to immobilize antigen. This amplification strategy may offer a simple and inexpensive platform for polycyclic aromatic hydrocarbons (PAHs) fast screening and on-line monitoring.

Keywords: Benzo[a]pyrene; Graphene; Poly(amidoamine) dendrimers; Electrochemical immunosensor

1. INTRODUCTION

PAHs are chemical compounds that consist of more than two fused aromatic rings in a linear or clustered arrangement. As a class of well-known carcinogenic compounds originating from incomplete

burning of oil, coal, gas and other organic materials, PAHs with lower molecular weight tend to be more concentrated in the vapor-phase while the ones with higher molecular weight are often associated with particulates [1]. Since benzo[a]pyrene (BaP) can make a consistent contribution to the total carcinogenic activity of the overall mixture of PAHs [2], researchers have analyzed BaP from different depth or height in water body, soil or air by HPLC, GC and GC-MS [3-5]. However, not only complex and time-consuming extraction in sample pretreatment and expensive equipment were needed, but also the low solubility of BaP limited their application.

Recently, basing on the sensitive and selective immuno-interaction between antibody and antigen, and simple pretreatment and fast response of the electrochemical transducer, the electrochemical immunosensor has been a facile and popular method to detect chemicals and biomolecules, especially using signal amplification including optimizing enzyme substrates [6], applying new redox-active probes [6], integrating layer-by-layer surface [7] or incorporating nanomaterials with proteins [8, 9]. Among these strategies, the nanoparticle-based amplification has attracted special interest. Especially, due to the large surface area, high conductivity, inherent carboxyl groups, electrochemical stablity and biocompatibility, carbon nanomaterials including carbon nanotubes, carbon nanofibers, carbon spheres and graphene are widely used in the surface modification and signal detection of immunosensors. As one of the most heated carbon materials, graphene sheets, with two-dimensional atomic thick sheets of sp^2 bonded carbon atoms [10], not only present an abundant domain for biomolecule binding in the sensor platform, but also play a role of fast electron-transfer in the electrochemical detection. As far as we know, most of graphene sheets used in biosensors were produced by the oxidation of graphite with strong oxidants, followed by the reduction of graphene oxides[11,12]. Except for dangerous oxidants such as concentrated sulfuric acid and potassium permaganate, the reduction of graphene oxides also decreased the functional groups such as carboxyl, carbonyl, hydroxyl on the surfaces and edges of graphene nanosheets[13]. Recently, a new and mild electrochemical sythesis of ionic-liquid- functionalized grephene from graphite was reported, which can not only preseve their schistose texture and functional groups without further reduction, but also increase the electrical conductivity by the inserting of the ionic-liquid into the nanosheets [14].

The involvement of nanomaterials can greatly amplify response signals of the immunosensor, however, the repeatablity of the immunosensor still requires a controllable and stable modification on the substrate. Compared with traditional methods, electrochemical deposition can be used to selectively deposite a film on the substrate with controllable thickness [15]. As one of the most promising biopolymers, chitosan(CS) is protonated and water soluble in a mildly acidic condition, while it is uncharged and insoluble in a basic condition [16], so it has been used to electrodeposit nanomaterials on the substrate, including chitosan-gold nanoparticles composites for acetylcholinesterase biosensor [17], chitosan-carbon nanofiber composites for cytosensing [18], chitosan-hematite nanotubes composites for hydrogen peroxide biosensor [19] and chitosan-carbon nanotubes-gold nanoparticles composite for carcinoma embryonic antigen (CEA) immunosensor [20], showing that such electrochemically-deposited chitosan-nanomaterial composite could be tightly attached to the electrode without changing their natural properties.

Furthermore, the sensitivity of electrochemical immunosensors is relative with the quantity of immuno-complexes. Nowadays, poly(amidoamine) dendrimers (PAMAM), with many functioal

groups outside the molecule [21] to immobilize biomolecules, have been extensively used in enzyme [22], antibody [23] or DNA aptamer [24] biosensors. Because of the positive charge of amino groups, PAMAM was often decorated onto the sensing surface by electrostatic adsorption [22, 24, 25]. For example, in the electrochemical detection of rutin, a graphene-chitosan film was directly dried onto the electrode surface, followed by adsorption of PAMAM[25]. However, PAMAM are quite soluble in water (amino groups are hydrophilic groups), and gradual elution of surface materials should be considered. Therefore, we use glutaraldehyde (GA) to perform a bridge between PAMAM and graphene-chitosan (GS-CS), which can not only be more stable and controllable, but also immoblize more antigens on the electrode surface due to the abundant amino groups.

In present work, graphene nanosheets were synthesized by a simple ionic-liquid-assisted electrochemical method, and characterized by fourier transform infrared spectrum (FT-IR) and transmission electron microscopy (TEM). Subsequently, a novel electrochemcial immunosensor was constructed by using the GS-CS electrodeposition film as a matrix and a multi-functionalized PAMAM to immobilize antigen, which were characterized by cyclic voltammetry (CV) and scanning electron microscopy (SEM). In a typical competitive immunoassay, the immobilized BaP-antigen (BaP-Ag) competed with free BaP in the solution to form an immuno-complex with antibody. Finally, the immunosensor was incubated with horseradish peroxidase labeled-secondary antibody (HRP-Ab_2) and the electrochemical signal was collected in a hydroquinone (HQ)/H_2O_2 system by CV. The optimization of the experimental conditions and the preformance of this immunosensor were studied in detail.

2. EXPERIMENTAL

2.1 Reagents and materials

Ctyl-3-methyl-imidazolium hexafluorophosphate was bought from Chengjie Chemical Company, Shanghai. BaP and 1-aminopyrene were bought from J&K Chemical Company. Polycyclic aromatic hydrocarbon antibody (Ab_1, 200 μg/ml) and goat anti-mouse IgG-HRP (HRP-Ab_2, 400 μg/ml) were from Santa Cruz. BaP-Ag was prepared using the diazotization method by the association of 1-aminopyrene with bovine serum albumin (BSA). PAMAM dendrimers were synthesized from a tetrafunctional core of ethylenediamine by successive addition of methyl acrylate and ethylenediamine according to the previous literature [26]. The dendrimer in this work was G2.0 with 16 amino groups on the outside of one molecule. All other reagents were of analytical grade and used without further purification.

In electrochemical experiments, phosphate buffers (PBS, 1/15 M) with different pH were used by mixing 1/15 M Na_2HPO_4 (containing 0.1 M KCl) and 1/15 M KH_2PO_4 (containing 0.1 M KCl) in different ratios. PBS buffer (pH 7.4, 0.01 M) was prepared by dissolving 8.5 g NaCl, 0.2 g KCl, 0.2 g KH_2PO_4 and 2.9 g $Na_2HPO_4{\cdot}12H_2O$ in 1 L water and used as a rinsing buffer in the immunosensor preparation. Furthermore, PBST (pH 7.4) was prepared by adding Tween 20 to PBS (pH 7.4, 0.01 M) at a final concentration of 0.05% (V/V). BaP stock solution was prepared by dissolving BaP powder in

acetonitrile at a concentration of 2×10^{-3} M and standard working solutions were prepared by diluting the stock solution with methanol.

2.2 Instruments

A model potentiostat (Guangzhou Weijie, China) was used to provide the static potential. The synthesized ionic-liquid-assisted graphene was characterized by FT-IR spectrum (FT-IR360, Nicolet, USA) and TEM (Tecnai 12, FEI, Holland). Morphologies of sensor surfaces were characterized by SEM (JEOL JIB-4600F, Japan). All electrochemical experiments were performed on CHI660C (Shanghai Chenhua Instrument, China) with a three-electrode system composed of the modified glassy carbon electrode as a working electrode, saturated Ag/AgCl electrode as a reference electrode and Pt electrode as an auxiliary electrode, respectively.

2.3 Synthesis of ionic-liquid-assisted graphene sheets

Graphene was synthesized using an ionic-liquid-assisted electrochemical method according to the previous literature [14]. Briefly, two high-purity graphite rods were parallelly placed with a separation of 4.0 cm in the 4.5 mL ionic liquid/water solution (V/V=1:1). Static potentials of 13 V were applied between two electrodes. After 6 h, the precipitate of the anode electrode was taken out, washed thoroughly with ethanol and water, and dried in an oven at 60 °C for 2 h.

2.4 Fabrication of functionalized graphene sheets platform

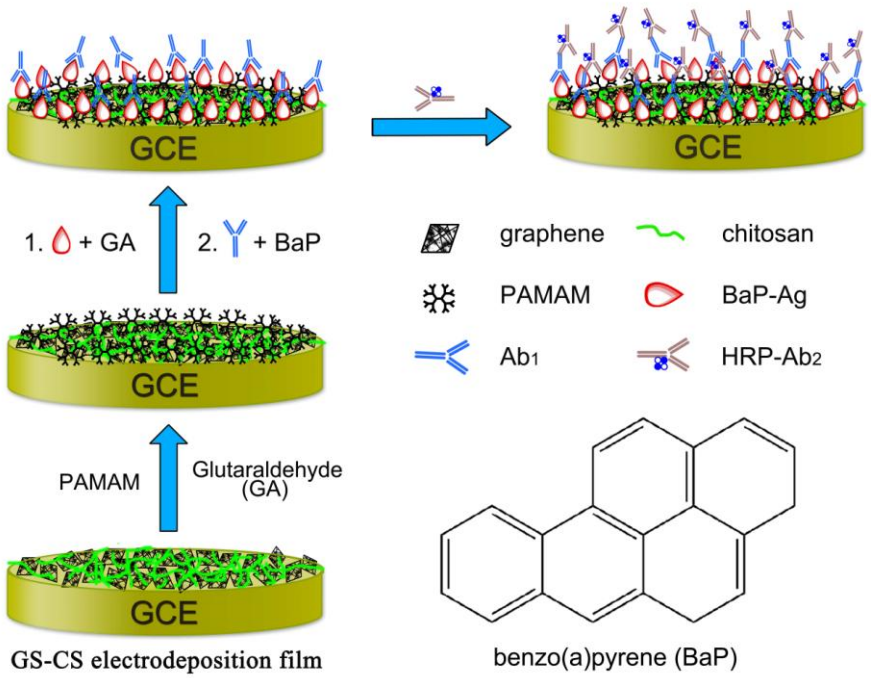

Scheme 1. Schematic illustration of the PAMAM/GS-CS immunosensor for BaP detection.

The GS-CS solution was prepared as following: (1) 0.1 g chitosan was dissolved in 8 mL of 2% HAc solution and 4 mg of graphene was ultrasonically dispersed in 2 mL of 2% HAc solution; (2) After the graphene solution was added into the chitosan solution, the mixture was sonicated for 20 min to obtain a homogeneous dispersion and stored at 4 °C when not in use.

The typical self-assembly construction of the immunosensor was shown in Scheme 1. Prior to the experiment, the glassy carbon electrode (GCE) was firstly polished to a mirror finish, followed by sonicating in dilute nitric acid, double distilled water and ethanol, respectively. Then, the electrodeposition was conducted in the GS-CS solution at an applied potential of -3.0 V for 600 s. After that, the GS-CS/GCE was washed with water to remove any free monomers. Then, 10 μL of 0.25% GA solution was dropped on the electrode surface to activate the surface amino groups of chitosan. After 1 h, the electrode was washed with water, followed by the inoculation of 10 μL of 5 mM PAMAM dendrimers (2.0 G) solution for another 1 h. After carefully washing with water, another 10 μL of 0.25% GA solution was dispersed on the surface to activate amino groups of PAMAM.

2.5 Immunoassay procedure for detection of BaP

For a typical experiment, the measurement protocol was described as follows. (1) The amino-activated PAMAM/GS-CS/GCE was incubated with 10 μL of BaP-Ag at 4 °C overnight, followed by washing with PBS buffer. (2) To avoid nonspecific binding, the modified electrode was then incubated in 4 mg/mL BSA solution for 1 h at 37 °C to block possible remaining active sites of PAMAM dendrimers. (3) 5 μL of BaP solution (with various concentrations) was mixed with 95 μL of Ab_1 in 0.01 M PBS (pH 7.4), followed by immediately incubating with the BaP-Ag/PAMAM/GS-CS/GCE platform. The electrode was firmly fixed and then kept at 37 °C for 1 h. (4) The electrode (Ab_1/BaP-Ag/ PAMAM/GS-CS/GCE) was incubated with 10 μL of HRP-Ab_2 solution at 37 °C for another 40 min, followed by washing with 0.01 M PBS (pH 7.4) to remove the nonspecific adsorption of free HRP-Ab_2. (5) Finally, the electrode was placed in an electrochemical cell containing 4 mL 1/15 M PBS (pH 7.4) and 1 mM HQ.

Cyclic voltammograms (CVs) were continuously recorded between -0.4 and 0.8 V after every 5 μL of 0.48 M H_2O_2 was injected for 4 times (final concentration: 2.4 mM), and the cathodic current change was used to characterize the immune response.

3. RESULTS AND DISCUSSIONS

3.1 Morphology characterization of the sensor platform

Fig. 1A showed FT-IR spectrum of ionic-liquid-assisted graphene sheets after carefully washing and drying. The C-H stretching vibration at 2920 cm^{-1} and 2860 cm^{-1}, the C-H deformation vibration at 1460 cm^{-1}, as well as the imidazolium framework vibration at 1640 cm^{-1} indicated the presence of ionic liquid groups. Fig. 1B was TEM image of the ionic-liquid-assisted graphene sheets,

which showed that the average length of the sample was up to 700 nm with a width of 500 nm, and some corrugations and scrollings on the edge of the graphene [14, 27].

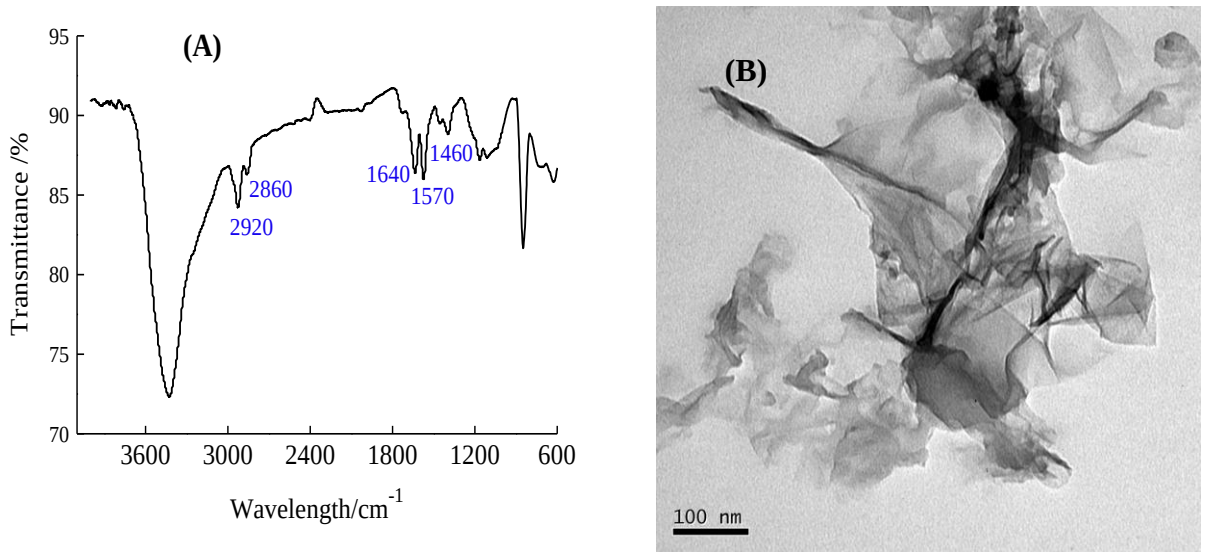

Figure 1. IR spectrum (A) and TEM image (B) of ionic-liquid-assisted graphene sheets

The morphologies of chitosan-electrodeposited electrode, and graphene/chitosan-electrodeposited electrode were characterized by SEM. Fig. 2A showed the directly electrodeposited chitosan film, indicating a uniform and leaves-like film on the electrode surface. Fig. 2B was SEM image for the graphene/chitosan electrodeposited film. Apparently, this nanocomposite film exhibited a highly compact surface with a three-dimensional structure and many paper-like graphene sheets were homogenously distributed in the film, indicating a nanocomposite film consisting of chitosan entrapped graphene was formed through this one-step electrodeposition process.

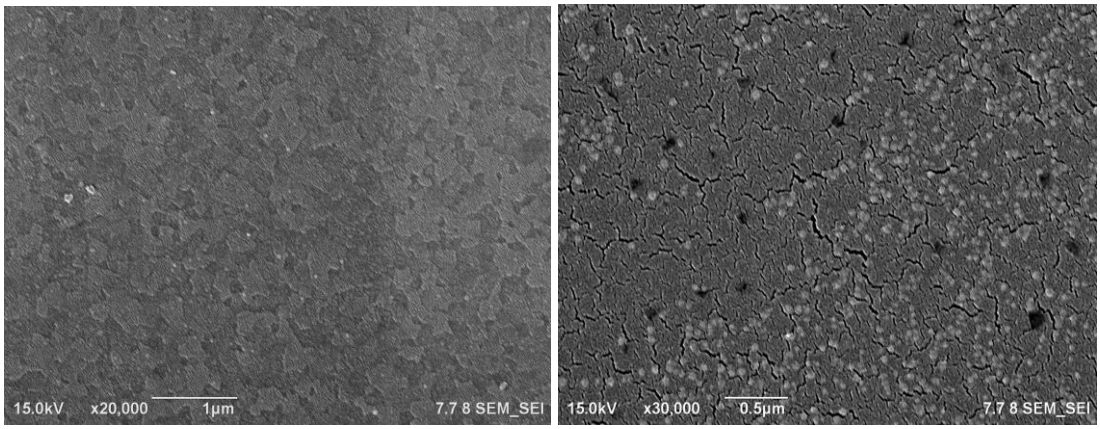

Figure 2. SEM images of chitosan-electrodeposited electrode (left) and graphene/chitosan-electrodeposited electrode (right)

3.2 Electrochemical characterization of the sensor platform

In the chitosan electrodepositon, if a reduction potential is applied, H^+ in the chitosan solution will reduced to H_2 and pH near the cathode surface gradually increased. Supposing that pH is higher than the pKa of chitosan, chitosan hydrogel can be locally electrodeposited onto the cathode surface [16]. In this work, with the aid of ionic-liquid-assisted graphene, a layer of graphene/chitosan was firstly electrodeposited on the surface, and PAMAM dendrimer was further linked with amino groups of chitosan by GA. To monitor each immobilization step, CV was performed in 1 mM $[Fe(CN)_6]^{3-/4-}$ containing 0.1 M KCl at a scan rate of 50 mV/s and the corresponding results were shown in Fig. 3. A couple of typical redox peaks for $[Fe(CN)_6]^{3-/4-}$ were appeared at the bare GCE with an anodic peak current of about 8.9 μA (Curve *a*). After chitosan was electrochemically deposited onto the surface, an increase in peak currents for $[Fe(CN)_6]^{3-/4-}$ was observed and the anodic peak current was about 12.1 μA (Curve *b*), the reason of which may be that the protonation of chitosan increased the penetration of $[Fe(CN)_6]^{3-/4}$.

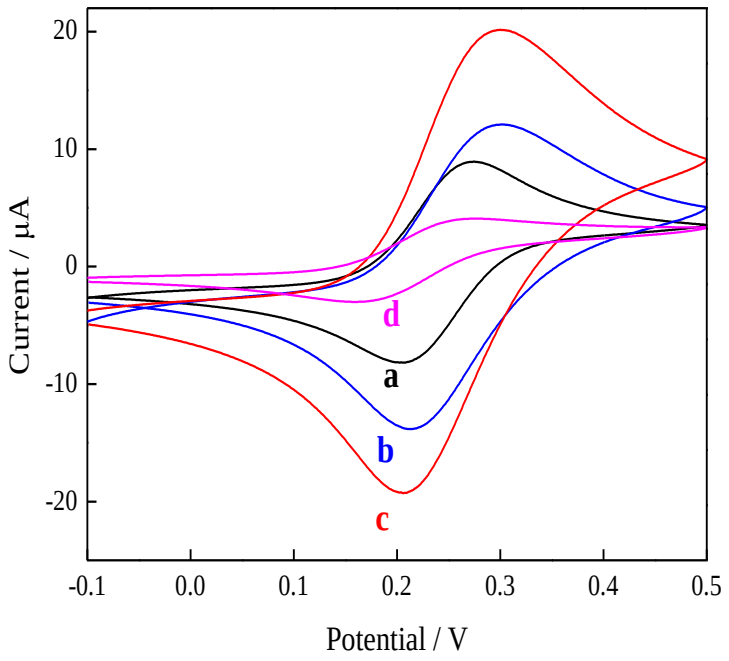

Figure 3. Cyclic voltammograms of bare GCE (a), chitosan-modified GCE (b), GS-CS- modified GCE (c) and PAMAM/GS-CS modified GCE (d) in 0.1 M KCl + 1 mM $K_3Fe(CN)_6/K_4Fe(CN)_6$ solution. Scan rate: 50 mV/s

However, if the electrodeposition was performed in the chitosan-graphene solution, the carboxyl and hydroxyl groups of graphene could interact with the reactive amino and hydroxyl functional group of chitosan to form a high dispersed GS-CS colloidal solution [16], thus a remarkable increase in the peak currents appeared and the anodic current was 20.2 μA (Curve *c*), about 1.7 times higher than that on the chitosan-modified electrode, indicating the successful doping of graphene. In

this way, the surface area of the electrode was enlarged by the nanostructure of ionic-liquid-assisted graphene/chitosan composite and the electron transfer rate of the platform was improved by the high conductivity of ionic-liquid-assisted graphene. In the CV for PAMAM/GS-CS/GCE (Curve *d*), the anodic peak current was 4.1 μA, greatly lower than the former electrodes, implying that the association of PAMAM hindered the electron transfer from the solution to the sensor surface due to their huge space structure.

3.3 Signal amplification strategy using dendrimer-enhanced graphene platform

As shown in the Scheme 1, the two-step amplification was based on using GS-CS composite as the sensor surface and PAMAM dendrimer (G 2.0) for antigen immobilization. To investigate the effect of PAMAM and graphene sheets, the BaP-Ag/GS-CS/GCE immunosensor (Fig. 4B) and the BaP-Ag/chitosan/GCE immunosensor (Fig. 4C) were designed, respectively. All these immunosensors were then incubated with Ab_1 and further labeled with HRP-Ab_2. Finally, the performance of these immunosensors was recorded in pH 7.4 PBS buffer containing 1 mM HQ in the absence or presence of 2.4 mM H_2O_2, respectively. As shown in Fig 4A, a pair of HQ redox peaks was observed with a cathodic current of -3.31 μA at -0.1 V (Curve *a*) for the PAMAM/GS-CS/GCE immunosensor. However, after the addition of H_2O_2, a dramatic decrease of the cathodic peak current was observed (Curve *b*). The possible catalytic mechanism by HRP may be described as the following:

$$\text{HRP } (Fe^{3+}) + H_2O_2 \rightarrow \text{Compound (I)} + H_2O \qquad (1)$$

$$\text{Compound (I)} + HQ \rightarrow \text{Compound (II)} + Q \qquad (2)$$

$$\text{Compound (II)} + HQ \rightarrow \text{HRP } (Fe^{3+}) + Q + H_2O \qquad (3)$$

$$Q + H^+ + 2e^- \rightarrow HQ \text{ (Electrode reaction)} \qquad (4)$$

where HQ is hydroquione and Q is the oxidation state of HQ. With the aid of H_2O_2, HRP is quickly oxidized to Compound (I), which could oxidize HQ to Q with a two-electron transfer process, causing a great increase in Q and the reduction peak.

Furthermore, the cathodic current for the BaP-Ag/GS-CS/ GCE immunosensor (Fig. 4B) and the BaP-Ag/chitosan/GCE immunosensor (Fig. 4C) was -5.76 and -10.23 μA before H_2O_2 addition, respectively, which was much higher than that on the PAMAM/GS-CS/GCE immunosensor. The reason may be that the introduction of graphene and PAMAM increased the amount of the antigen on the sensor surface, which can hinder the electron transfer of HQ on the electrode surface. However, after the addition of H_2O_2, the cathodic current was changed as -7.78, -8.73 and-12.32 μA, respectively. Using the current change (ΔI) of the cathodic peak before (*a*) and after (*b*) the addition of H_2O_2 as the detection signal, it can be deduced that ΔI of the BaP-Ag/GS-CS/GCE immunosensor (Fig. 4B) was 1.42 times that of the BaP-Ag/CS/GCE immunosensor (Fig. 4C),

indicating the large specific surface area of ionic-liquid-assisted graphene greatly increased the active area of the platform and its conductivity enhanced the electron transfer among chitosan, HRP and the electrode surface [28, 29]. In addition, compared with the BaP-Ag/GS-CS/GCE immunosensor (Fig. 4B), the response of the BaP-Ag/PAMAM/GS-CS/GCE immunosensor (Fig. 4A) was 1.51 times higher; indicating the addition of PAMAM can largely improve the signal intensity. Therefore, it can be concluded that the existence of ionic-liquid-assisted graphene and PAMAM significantly amplify the detection signal and further improve the sensitivity of the immunosensor.

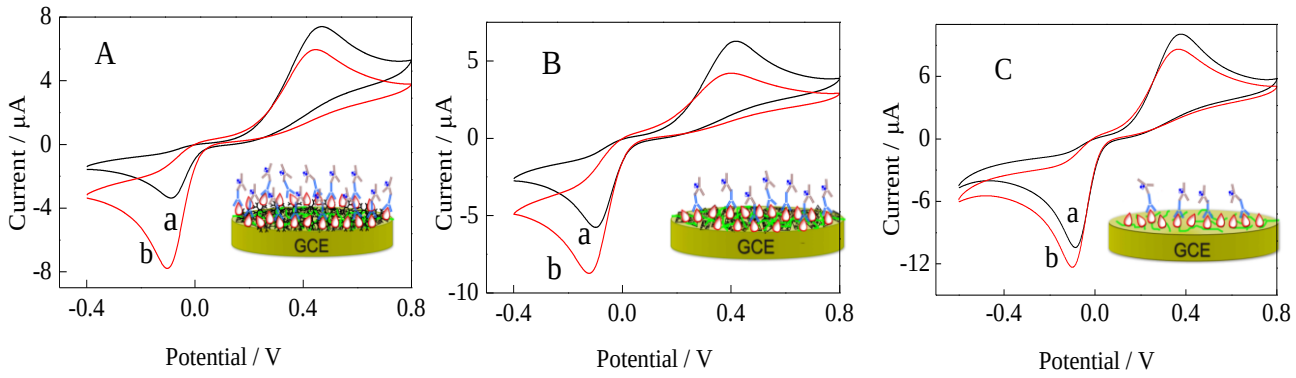

Figure 4. Cyclic voltammograms of HRP-Ab_2/Ab_1/BaP-Ag/PAMAM/GS-CS/GCE (A), HRP-Ab_2 /Ab_1/BaP-Ag/GS-CS/GCE (B) and HRP-Ab_2 /Ab_1/BaP-Ag /chitosan/GCE (C) in 4 ml of PBS buffer (pH 7.4) containing 1 mM HQ before (*a*, black) and after (*b*, red) the addition of 2.4 mM H_2O_2

3.4 Optimization of detection conditions

The electrochemical signal of enzyme-based immunosensor depended on the catalysis reaction of the enzyme. In addition, a suitable electrochemical condition can improve the electron transfer rate at the electrode. Therefore, by investigating the relationship between the signal response and the concentration of biomaterial (antigen, Ab_1 or Ab_2) bulk solution, the pH of the buffer, optimum conditions in immunoassay were obtained.

In the optimization of BaP-Ag concentration, the dilution ratio of Ab_1 was fixed at 200:1 (PBS: Ab_1) while the dilution ratio of BaP-Ag was altered from 40:1 to 200:1 (PBS: BaP-Ag). The signal response of the immunosensor gradually increased with the ratio from 80:1 to 200:1, but it sharply decreased if the ratio was smaller than 80:1. The compromise between the largest immobilization capacity of BaP-Ag and the accompanying stereo-hindrance effect should be adopted, so the ratio of 80:1 was selected in the subsequent research (Fig. 5A).

In the optimization of Ab_1 concentration, the dilution ratio of BaP-Ag was fixed at 80:1 and the dilution ratio of Ab_1 was investigated between 1000:1 and 100:1. As shown in Fig. 5B, the current response showed a linear relationship with the dilution ratio of Ab_1 in the range of 600 to 200, indicating a fine platform for competitive immunoassay. Thus the optimal dilution ratio of Ab_1 was selected as 600:1 in the following steps.

The effect of buffer pH on the behavior of the immunosensor was investigated over a pH range from 4.9 to 9.2. As shown in Fig. 5C, it can be observed that the current response increased from pH 4.9, reached the maximum value at pH 7.4 and then decreased to pH 9.2. It was known that the stability of chitosan film decreased in strong acidic medium. In addition, from Eqn. 4, a higher pH may promote the reaction rate of HRP with H_2O_2. However, if the pH was higher than 7.4, HQ may be easily oxidized to benzoquinone. Hence, pH 7.4 was fixed as the operating pH of HQ solution in subsequent experiments

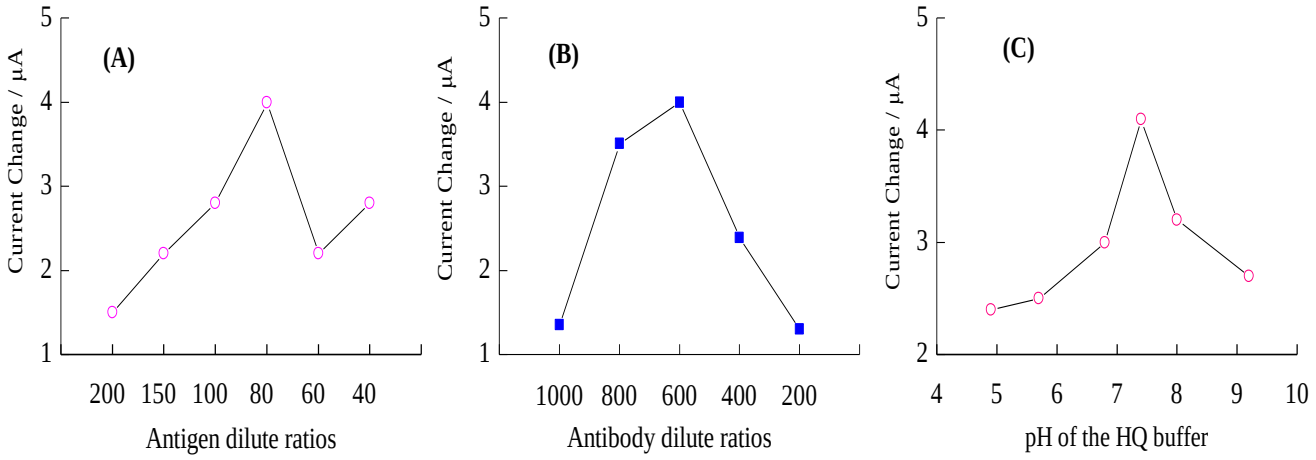

Figure 5. Effect of BaP-Ag concentration (A), Ab_1 concentration (B) and pH of the buffer solution (C) on the immunosensor current response in the presence of 2.4 mM H_2O_2

3.5 Immuno-detection of BaP using the PAMAM/GS-CS/GCE immunosensor

For the BaP measurement, a competitive assay was applied under optimized conditions, that is to say, a series of BaP solutions competed with the immobilized BaP-Ag on the sensor surface to bind the limited binding sites of the Ab_1. After the immunoreaction with HRP-Ab_2, CVs of the immunosensor were measured in the mixture of 1 mM HQ and 2.4 mM H_2O_2 (Fig. 6A), showing that the absolute value of the cathodic current decreased with the increase in BaP concentrations. Using the reduction current change (ΔI) before and after the addition of H_2O_2, the relationship between ΔI and BaP concentrations at -0.1 V can be found in Fig. 6B. Furthermore, from the inset of Fig. 6B, a linear relationship between ΔI and $\lg C_{BaP}$ was exhibited in the range from 5 nM to 6 μM and a detection limit was estimated at 3 nM (S/N=3). The regression equation was y = 2.02-1.14 x with a correlation coefficient of 0.987, where y and x represented ΔI and $\lg C_{BaP}$, respectively. In earlier work, a complex two-step concentration was used to enrich BaP and a UV-detection capillary electrophoresis was used to detect BaP in the range of 6.4 nM and 0.8 μM with a detection of 1.6 nM [30]. Furthermore, a thiolated hapten-modified gold electrode was applied for voltammetric immuno-analysis of BaP in the range of 0.1 and 5 μM [31], while a ruthenium tris(bipyridine)-pyrenebutyric acid conjugate was used as a redox-labeled tracer for the electrochemical immunoassay of BaP with a detection limit of 10 nM

[32] and a disposable screen-printed carbon immunosensor was used to detect phenathrene with a detection limit of 2 ng/ml [33], respectively. The performance of the proposed immunosensor was comparable with or better than previously reported BaP or PAH immunosensors, resulting from the dual-amplification of ionic-assisted graphene and PAMAM.

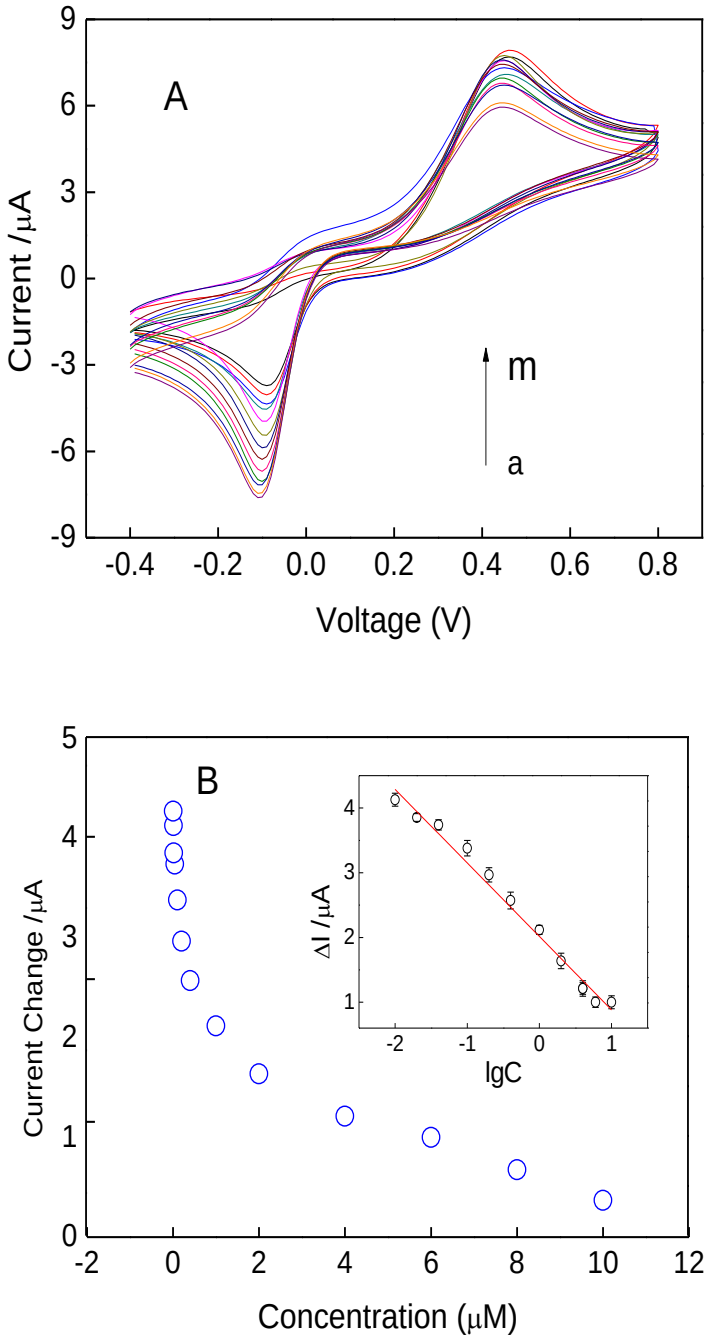

Figure 6. Cyclic voltammograms of the BaP-Ag/PAMAM/GS-CS/GCE immunosensor at different BaP solutions with concentrations of 0.005, 0.01, 0.02, 0.04, 0.1, 0.2, 0.4, 1.0, 2.0, 4.0, 6.0, 8.0, 10.0 μM (from *a* to *m*) in PBS buffer (pH 7.4) containing 1 mM HQ and 2.4 mM H_2O_2 at a scan rate of 100 mV/s (A). The relationship between current changes and BaP concentrations (B). Inset: the linear fitting between current changes with the logarithm of BaP concentrations (*N* = 3)

3.6 Reproducibility and stability of the immunosensor

The reproducibility of the immunosensor was estimated by intra-assay of variations. The intra-assay precision was evaluated by assaying one level of BaP for three parallel measurements on the same immunosensor. As shown in Fig. 6B, the immunosensor precision was displayed by calculating the average value of relative standard deviation (RSD) for all experiments. The average value of RSD was about 9.6%, suggesting the precision and reproducibility of the proposed immunosensor was acceptable.

The long-term stability of the BaP-Ag/PAMAM/GS-CS/GCE immunosensor was examined. The sensor was stored at 4 °C when not in use. After 48 h, the current response of the immunosensor retained about 96.5% of the initial intensity, indicating that the PAMAM/GS-CS film could provide a biocompatible microenvironment for the bimolecule immobilization.

3.7 Real sample analysis

To examine the applicability and reliability of the present immunosensor for practical analysis, recovery experiments were performed by standard addition method in the water from Poyang Lake in South China Agriculture University. Several standard samples were added into the water to prepare BaP concentrations of 0.02, 0.05, 0.1, 0.5 and 2.0 μM. The experimental results were listed in Table 1, showing an acceptable recovery in the range of 96% and 110%. This also indicated that the present immunosensor might provide an alternate method for determining BaP or other contaminants in environmental pollutants.

Table 1. Recovery of the prepared immunosensor in water

Sample	Standard value of BaP (μM)	Found (μM)	Recovery (%)
1	0.02	0.022	110
2	0.05	0.048	96
3	0.1	0.102	102
4	0.5	0.51	102
5	2.0	1.98	99

4. CONCLUSIONS

In this work, a novel strategy for the construction of BaP immunosensor was developed based on the immobilization of antigen on the PAMAM modified one-step ionic-assisted-graphene/chitosan nanocomposite film. The large specific surface area of ionic-assisted-graphene sheets can increase the active area of the platform and its conductivity could enhance electron transfer among chitosan, the

active center of HRP and the electrode surface, while the present of PAMAM dendrimer greatly enhanced the immobilized ability of BaP-Ag by providing more amino-groups as binding sites. The proposed BaP immunosensor exhibited a relatively wide linear range between 5 nM and 10 μM with a detection limit of 3 nM, fine reproducibility and stability. The simple fabrication procedure and the sensitivity may provide great potential for PAHs fast screening and on-line monitoring in environmental applications.

ACKNOWLEDGEMENTS
The authors thank the financial support of Natural Science Foundation of China (21105030), the National Basic Research Program of China (2009CB421601), the Student Innovative Project of Guangdong Province (105641003) and the Key Academic Program of 211 Project of South China Agricultural University (2009B010100001).

References

1. K. Ravindra, E. Wauters and R. Van Grieken, *Sci. Total. Environ.*, 396 (2008)100
2. M. Piñeiro-Iglesias, G. Grueiro-Noche, P. López-Mahía, S. Muniategui-Lorenzo and D. Prada-Rodríguez, *Sci. Total. Environ.*, 334-335 (2004) 377
3. A.H.W. Abdulkadar, A.A.M. Kunhi, A. Jassim and A. Abdulla, *Food Addit. Contam.*, 20 (2003) 1164
4. S.F. Aygün and F. Kabadayi, *Int. J. Food Sci. Nutr.* 56 (2005) 581
5. T.T.T. Dong and B.K. Lee, *Chemosphere*, 74 (2009) 1245.
6. M.R. Akanda, M.A. Aziz, K. Jo, V. Tamilavan, M.H. Hyun, S. Kim and H. Yang, *Anal. Chem.*, 83 (2011) 3926.
7. R. Chai, R. Yuan, Y.Q. Chai, C.F. Ou, S.R. Cao and X.L. Li, *Talanta*, 74 (2008) 1330
8. J. Tang, D.P. Tang, R. Niessner and D. Knopp, *Anal. Bioanal. Chem.*, 400 (2011) 2041.
9. J. Pan and Q.W. Yang, *Anal. Bioanal. Chem.*, 388 (2007) 279
10. K.S. Novoselov, A.K. Geim, S.V. Morozov, D. Jiang, Y. Zhang, S.V. Dubonos, I.V. Grigorieva, and A.A. Firsov, *Science*, 306 (2004) 666
11. Q. Wei, K. Mao, D. Wu, Y. Dai, J. Yang, B. Du, M. Yang and H. Li, *Sens. Actuat. B*, 149 (2010) 314.
12. Y.Y. Shao, J. Wang, H. Wu, J. Liu, I.A. Aksay and Y.H. Lin, *Electroanalysis*, 22 (2010)1027
13. Y. Li, W. Gao, L. Ci, C. Wang and P.M. Ajayan, *Carbon*, 48 (2010) 1124
14. N. Liu, F. Luo, H.X. Wu, Y.H. Liu, C. Zhang and J. Chen, *Adv. Funct. Mater.*, 18 (2008) 1518
15. P.N. Deepa, M. Kanungo, G. Claycomb, P.M.A. Sherwood and M.M. Collinson, *Anal. Chem.*, 75 (2003) 5399
16. L.Q. Wu, A.P. Gadre, H. Yi, M.J. Kastantin, G.W. Rubloff, W.E. Bentley, G.F. Payne and R. Ghodssi, *Langmuir*, 18 (2002) 8620
17. D. Du, J.W. Ding, J. Cai and A.D. Zhang, *J. Electroanal. Chem.*, 605 (2007) 53
18. C. Hao, L. Ding, X.J. Zhang and H.X. Ju, *Anal. Chem.*, 79 (2007) 4442
19. J.M. Gong, L.Y. Wang, K. Zhao and D.D. Song, *Electrochem. Commun.*, 10 (2008) 123
20. X. Gao, Y.M. Zhang, Q. Wu, H. Chen, Z.C. Chen and X.F. Lin, *Talanta*, 85 (2011)1980
21. E. Bustos and L.A. Godinez, *Int. J. Electrochem. Sci.*, 6 (2011) 1
22. J.C. Forti, S.A. Neto, V. Zucolotto, P. Ciancaglini and A.R. de Andrade, *Biosens. Bioelectron.*, 26 (2011) 2675
23. L. Svobodová, M. Šnejdárková, V. Polohová, I. Grman, P. Rybár and T. Hianik, *Electroanalysis*, 18 (2006) 1943

24. S. Koda, Y. Inoue and H. Iwata, *Langmuir*, 24 (2008) 13525
25. H.S. Yin, Y.L. Zhou, L. Cui, T. Liu, P. Ju, L.S. Zhu and S.Y. Ai, *Microchim. Acta*, 173 (2011) 337
26. B. Devarakonda, R.A. Hill and M.M. de Villiers, *Int. J. Pharm.*, 284 (2004) 133
27. H.F. Yang, C.S. Shan, F.H. Li, D.X. Han, Q.X. Zhang and L. Niu, *Chem. Commun.*, (2009) 3880
28. K.J. Huang, D.J. Niu, J.Y. Sun, X.L. Zhu and J.J. Zhu, *Anal. Bioanal. Chem.*, 397 (2010) 3553
29. W. Sun, X. Li, Y. Wang, R. Zhao and K. Jiao, *Electrochim. Acta*, 54 (2009) 4141
30. Y. Takagai and S. Igarashi, *Analyst*, 126 (2001) 551
31. M. Liu, Q.X. Li and G.A. Rechnitz, *Electroanalysis*, 12 (2000) 21
32. M.Y. Wei, S.D. Wen, X.Q. Yang and L.H. Guo, *Biosens. Bioelectron.*, 24 (2009) 2909
33. K.A. Fähnrich, M. Pravda and G.G. Guilbault, *Biosens. Bioelectron.*, 18 (2003) 73